ORIGINAL PAPER

Selective Oxidation of Chromium by O_2 Impurities in CO_2 During Initial Stages of Oxidation

**Soraya Bouhieda · Fabien Rouillard ·
Vincent Barnier · Krzysztof Wolski**

Abstract   This study shows that the corrosion behaviour of 12 wt% Cr steel in CO_2 at 550 °C is determined in the first stage of oxidation by reaction with O_2 impurities. Depending on the amount of theses impurities and the thermal ramp rate, selective oxidation of chromium could lead to the formation of a protective chromium-rich oxide. An oxidation model describing qualitatively the nature of the oxide layer formed in the initial period of oxidation is presented. From these observations, surface engineering processes for protecting 9–12 wt% chromium steels from fast corrosion rate have emerged.

Keywords   Ferritic–martensitic steels · Carbon dioxide · Selective oxidation · Impurity · Oxygen

Introduction

In the framework of the development of sodium fast reactors in France, carbon dioxide integrated in the Brayton cycle is proposed as new cycle energy conversion

S. Bouhieda · F. Rouillard (✉)
Laboratoire d'Etude de la Corrosion Non Aqueuse, CEA, DEN, DPC, SCCME,
91191 Gif-sur-Yvette, France
e-mail: fabien.rouillard@cea.fr

S. Bouhieda
e-mail: soraya.bouhieda@cea.fr

V. Barnier · K. Wolski
Laboratoire Claude Goux, UMR CNRS 5146, Centre SMS, Ecole des Mines de Saint-Etienne,
158 cours Fauriel, 42023 Saint-Etienne, France
e-mail: barnier@emse.fr

K. Wolski
e-mail: wolski@emse.fr

system to replace current steam generators. The main advantages of this cycle are the improvement of the reactor safety by suppressing the risk of the exothermic water–sodium reaction, the improvement of the cycle compactness and the increase of the cycle efficiency. Ferritic–martensitic (F/M) steels with 9–12 wt% Cr are good candidates for heat exchanger application for many reasons: they have good mechanical properties up to 650 °C, high thermal conductivity, low expansion coefficient and usually a lower cost as compared to austenitic steels. However, many studies have shown that their corrosion behaviour in CO_2 at 550 °C can dramatically affect their performance due to fast corrosion kinetics and strong carburization [1–9]. Few studies on the effect of the impurities present in CO_2 on the corrosion behaviour were presented in the literature and it can be pointed out that only the effect of a high amount of oxygen (1–3 %) in CO_2 was presented [10]. This study is interested in the effect of the impurities present in small amount (ppm) in CO_2 gas on the corrosion behaviour. Indeed, it was shown in a previous article that impurities present in carbon dioxide strongly impact on the corrosion behaviour from the initial stages of oxidation [11] and that depending on the CO_2 purity slow growing oxide scale could be formed on these F/M steels. In this study the impurity responsible for the corrosion behaviour of a 12 wt% Cr ferritic–martensitic steel (VM12) has been identified and discussion about phenomenon which could explain the transition from a thick iron rich oxide layer to a thin chromium rich oxide layer is presented. Particular attention was paid to the first stage of oxidation where the competitive formation of iron and chromium oxides starts.

Experimental Procedures

Materials

The 12 wt% Cr ferritic–martensitic steel (VM12) used in the corrosion tests was obtained from Vallourec and Mannesmann and the chemical composition of this material was in wt%: 11.5 Cr, 0.12 C, 0.49 Si, 0.35 Mn, 0.018 P, 0.001 S, 0.29 Mo, 0.29 Ni, 0.008 Al, 0.05 Nb, 0.26 V, 0.067 N, 1.62 Co, 0.005 B, 1.5 W. Samples were polished by standard mechanical polishing methods with grinding paper grades: 500, 1,200 then smoothed with 1 μm diamond paste to get mirror finish. Samples were ultrasonically degreased in a mixture of acetone and ethanol (1:1).

Gas

The different bottles of CO_2 used in the corrosion tests were provided by MESSER® and their compositions are presented in Table 1. Helium 6.0 gas was also used in order to study the effect of the carrier gas on the reactivity of impurities.

Corrosion Tests and Methods of Surface Analysis

The corrosion experiments were carried out in a tubular furnace with a gas flow rate of ∼40 L/h corresponding to 0.45 cm/s at atmospheric pressure. Very short-term

Table 1 Composition of the gas phase used in this study

Composition	CO$_2$ vol (%)	He vol (%)	O$_2$ (ppmv)	H$_2$O (ppmv)	N$_2$ (ppmv)	HC (ppmv)	CO (ppmv)
CO$_2$ 4.5	99.995	–	10	5	25	1	1
CO$_2$ 5.5	99.9995	–	1	–	2	0.5	0.5
He 6.0	–	99.9999	0.5	0.5	0.5	0.1	0.1

corrosion tests lasting only the duration of the thermal ramp up to 550 °C were carried out under different purity of CO$_2$ and under He 6.0. Furthermore, similar corrosion test under CO$_2$ with added ^{18}O$_2$ impurities thanks to a micro-leak valve were carried out in order to follow ^{18}O$_2$ reactivity in CO$_2$. Then, corrosion tests under different thermal ramp rates were performed in order to study the influence of this parameter on corrosion behaviour. The oxygen partial pressure of the gas phase was measured by an electrochemical oxygen probe using zirconia. Dedicated works on this oxygen probe on specific gas mixtures containing known amounts of CO, CO$_2$ and O$_2$ have shown that the measured value corresponds to the equilibrium oxygen partial pressure between all the gas species. When the amount of O$_2$ impurities is in large excess as compared to the amount of CO impurities, the oxygen probe can be identified as dedicated probe for O$_2$ impurities in the gas phase.

Finally, an accurate study of the initial stage of oxidation was carried out in X-ray photoelectron spectroscopy (XPS) apparatus ThetaProbe with a monochromatic Al Kα X-ray source and a UHV system at 10^{-9} m bar oxygen partial pressure. This experiment was conducted in order to identify the nature of the first oxide layers formed during the oxidation process. The following Table 2 shows different corrosion tests carried out with associated experimental parameters.

After each corrosion test, the distribution of elements in the scale was determined by glow discharge optical emission spectroscopy (GDOES) using Jobin–Yvon 50 model in radio-frequency mode.

Ion mass spectrometry (SIMS) analyses were performed on sample oxidized under CO$_2$ with added ^{18}O$_2$ impurities using a CAMECA-IMS 4F apparatus.

Results and Discussion

Influence of the Gas Purity

The sample oxidised during test 1 (CO$_2$ 4.5) presented a dark homogeneous oxide whereas the sample oxidized during test 2 (CO$_2$ 5.5) presented a thin oxide with yellowish reflection. On Fig. 1 are presented GDOES profile of the samples after test 1 and 2.

In Fig. 1a, the oxide layer formed under CO$_2$ 4.5 was a duplex oxide layer composed by an external oxide layer only made of iron (about 40 at.%) and by an internal iron–chromium oxide layer (about 13 at.% Cr). The GDOES profile of the

Table 2 Experimental parameters of the corrosion tests

	Surface finishing	Gas	Measured PO_{2eq} (ppm)	Thermal ramp rate to 550 °C	Gas flow rate (L/h)
Test 1	P1200	CO_2 4.5	70	2 °C/min	40
Test 2	P1200	CO_2 5.5	0.4	2 °C/min	40
Test 3	P 1 μm	CO_2 5.5 + 40 ppm $^{18}O_2$	40	2 °C/min + 1 h at 550 °C	40
Test 4	P1200	He +0.4 ppm O_2	0.4	2 °C/min	40
Test 5	P1200	He +136 ppm O_2	136	2 °C/min	40
Test 6	P1200	CO_2 4.5	70	15 °C/min	40
Test 7	P1200	He 6.0	0.4	15 °C/min	40
Test 8	P 1 μm	UHV (10^{-9} m bar)		2 °C/min	/
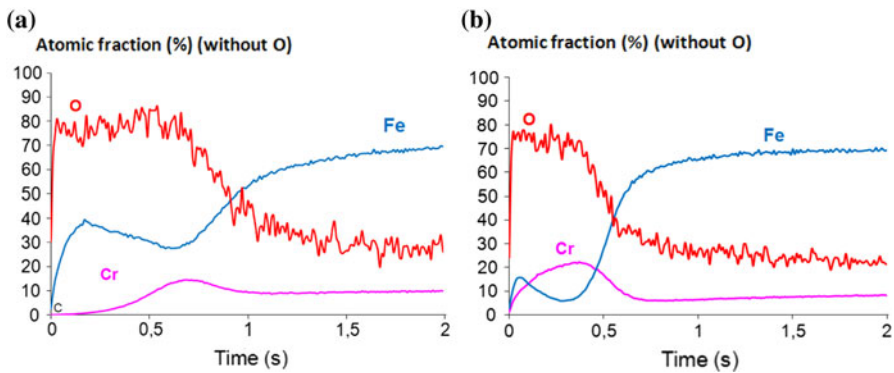
Fig. 1 GDOES profiles of samples oxidised at 2 °C/min from room temperature up to 550 °C under CO_2 4.5 (**a** test 1), and CO_2 5.5 (**b** test 2)

sample oxidised under CO_2 5.5 presented in Fig. 1b was very different. The oxide was still duplex but with the presence of chromium in the external oxide layer and an internal oxide layer richer in chromium (about 20 at.%).

As O_2 impurities present in the gas phase were the major species whose amount strongly differed between CO_2 4.5 and CO_2 5.5, it was assumed that the amount of O_2 impurities present in CO_2 was responsible for the corrosion behaviour modification. In order to check this assumption, test 3 (CO_2 5.5 enriched with 40 ppm of $^{18}O_2$) was carried out. $^{18}O/(^{18}O + ^{16}O)$ ratio obtained from SIMS profiles of the oxide layer built after test 3 is shown in Fig. 2a. The result was compared to the natural isotopic ratio of $^{18}O_2$ obtained by forming an oxide layer under $^{16}O_2$ containing CO_2 gas (Fig. 2b, test 2). Moreover SIMS profile of chromium is presented in order to identify the metal-oxide interface (Fig. 2c).

A strong ^{18}O enrichment in the oxide scale could be observed in Fig. 2a: the addition of only 40 ppm of $^{18}O_2$ in CO_2 led to 4 % enrichment of ^{18}O in the oxide scale (factor 1,000) which is much higher than the natural isotopic ratio 0.2 %, as illustrated by Fig. 2b. As a consequence, we may say that O_2 reactivity was at least
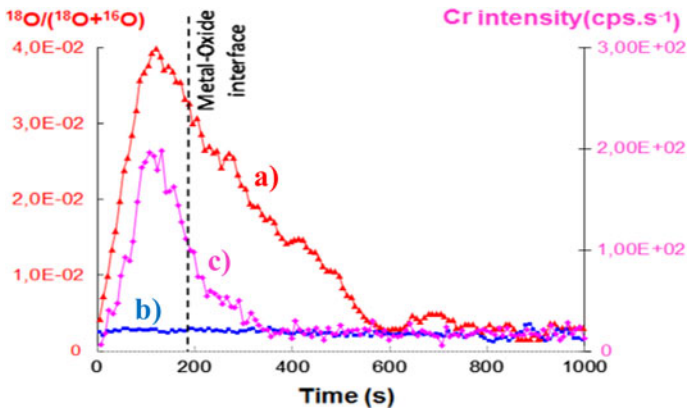
Fig. 2 $^{18}O/(^{18}O + ^{16}O)$ ratio obtained from SIMS profiles after corrosion test under *a* CO_2 5.5 + 40 ppm $^{18}O_2$ (test 3), *b* CO_2 5.5 containing 0.4 ppm $^{16}O_2$ (test 2), and *c* SIMS profile of Cr after test 3

one thousand times stronger than CO_2 reactivity. Furthermore, it can be noticed that this enrichment appeared to be more important close to the metal-oxide interface, which suggests either the strong reactivity of $^{18}O_2$ during the formation of the first oxide layers or an anionic growth of the oxide scale. In our study it is admitted that this enrichment is due to the reactivity of ^{18}O because of cationic growth of a rich chromium oxide layer. Then the decrease of the $^{18}O_2$ amount in the external part of the oxide layer might be due to a decrease of selectivity between $^{18}O_2$ and $C^{16}O_2$ reactions. Moreover, it could be noticed the presence of oxygen in the metallic substrate just below the metal-oxide interface, which may suggest internal oxidation. It should be pointed out that only 4 % of the oxygen present in the oxide layer is ^{18}O. If O_2 would have formed the whole thin oxide layer, the $^{18}O_2$ content of the oxide layer would have reached 100 % in theory. The authors think that the lower measured level of $^{18}O_2$ is not due to an important CO_2 reaction but to the fact that O_2 impurities injected into CO_2 were not completely $^{18}O_2$ and that a non negligible amount of ^{16}O coming from residual air in the pipe could have participated to the oxide layer formation. A similar test with a better control of $^{18}O_2$ level in the gas phase should be carried out again.

According to these results, the amount of O_2 impurities present in the CO_2 has appeared to have a strong influence on the nature of the first oxide layer formed. In order to identify the effect of CO_2 during the initial stages of oxidation, test 4 and 5 under He 6.0 containing two different amounts of O_2 impurities were carried out. The GDOES profiles of the samples after corrosion test 4 and 5 are presented on Fig. 3.

The oxide layer formed under He 6.0 with a low amount of O_2 (Fig. 3a) was composed by a duplex oxide layer with a very thin external oxide layer rich in iron with some chromium and an internal oxide layer rich in chromium (about 20 at.%). This oxide was similar to the one formed under CO_2 5.5 (Fig. 1b). By increasing the amount of O_2 impurities in the gas phase (Fig. 3b), GDOES profiles revealed the strong oxidation of iron: the oxide layer was duplex and composed by an external
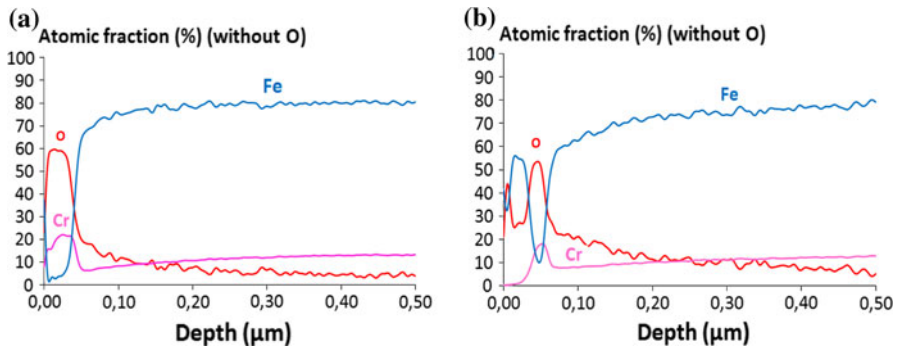
Fig. 3 GDOES profiles of samples oxidised at 2 °C/min from room temperature up to 550 °C under He 6.0 + 0.4 ppm O_2 (**a** test 4) and He 6.0 + 136 ppm O_2 (**b** test 5)

iron rich oxide layer (about 55 at.%), similar to the one formed under CO_2 4.5 (cf. Fig. 1a). However it could be noticed an important chromium enrichment in the internal iron–chromium oxide in contrary to the oxide formed under CO_2 4.5 (Fig. 1a). This difference will not be explained in this paper but, according to the authors, may be due to a different oxide growth mechanism in He–O_2 and CO_2.

To summarize the different results obtained from the corrosion tests, O_2 in the gas phase was responsible for the formation of the first oxide layers and depending on its amount in the gas phase, either an external iron oxide or an external iron and chromium oxide scale could be formed.

The aim of the next part is to understand why the oxide scale was richer in chromium when the amount of oxygen in the gas phase during the first stages of oxidation was low. As carbon dioxide was assumed to be inert in the first stage of oxidation, sample was only exposed to oxygen. An accurate study of the composition of the native oxide and its changing during the initial stage of oxidation under low amount of O_2 was carried out by in situ XPS oxidation.

Characterization of the Surface by In Situ XPS Oxidation Test

An accurate analysis of the oxide present on the sample before and after annealing from room temperature up to 550 °C at 2 °C/min under ultra high vacuum ($P < 10^{-9}$ m bar, test 8) in XPS facility containing an in situ furnace was carried out. This environment was assumed to be mainly composed by O_2 [12]. Mass transfer calculations considering gas kinetics theory have shown that the supply of oxygen to the surface is similar to the one obtained under 1 ppm O_2 in CO_2 at atmospheric pressure (considering mass transfer in diluted gas) [13]. In Fig. 4 is presented the XPS spectra of the oxide recorded at room temperature and after test 8.

On the general spectra presented in Fig. 4a, one could observe that the elements identified on the surface (at room temperature) were: Fe, Cr, O, N, Ca, C and Si. The surface was covered by a native oxide film and by impurities which could come from atmospheric pollution and/or human manipulation (C, Ca). After heating at 550 °C, the composition of the surface changed: a new oxide layer whose composition was
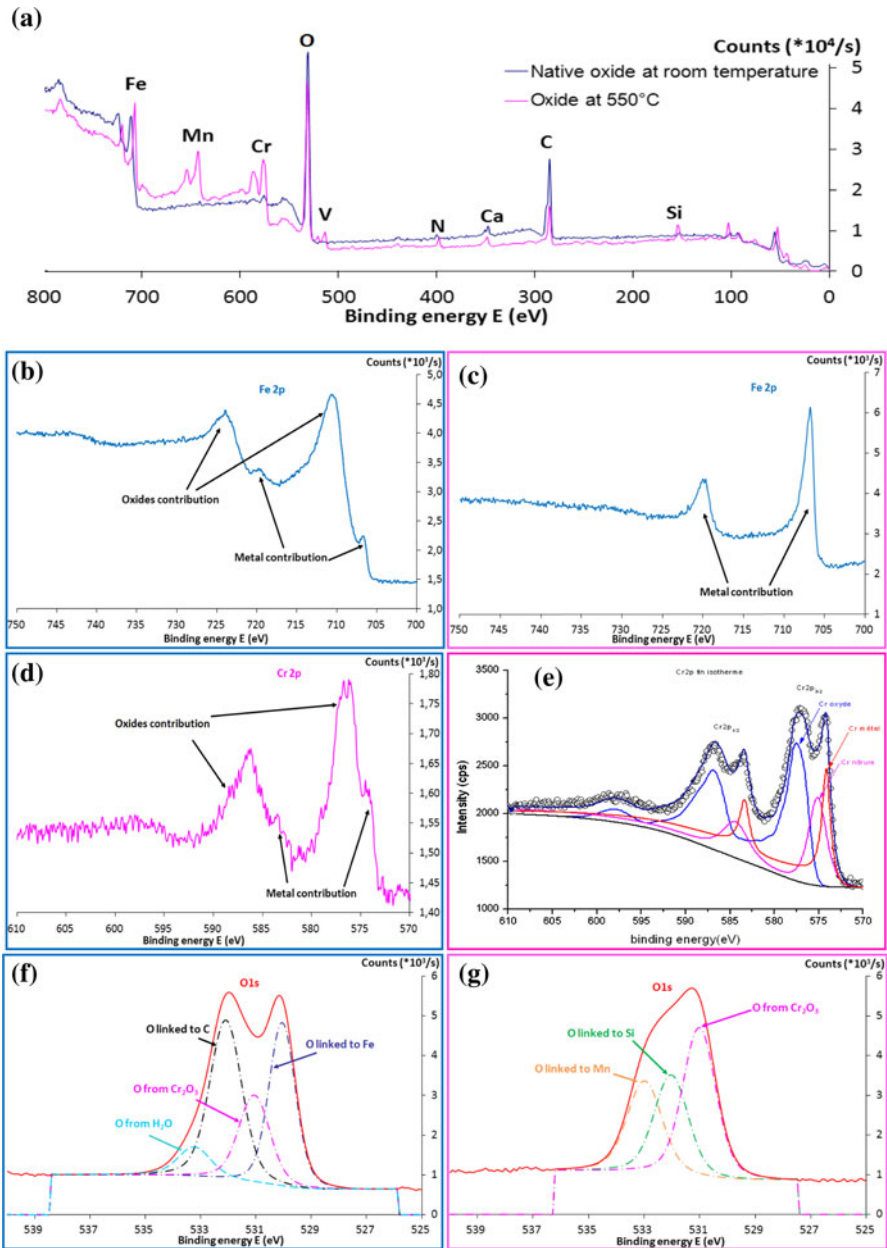
Fig. 4 General XPS spectra recorded at room temperature and at 550 °C on VM12 (**a**), XPS detailed spectra recorded at room temperature (**b**, **d**, **f**) and at 550 °C (**c**, **e**, **g**)

different from the native oxide film formed. Indeed, the surface was enriched in Cr, Mn, and Si. In order to have more information on the nature of the chemical bonds formed, high resolution spectra focused on Fe, Cr and O were recorded (Fig. 4b–g).

The detailed spectra focused on Fe and Cr (Fig. 4b, d) recorded at room temperature revealed that the peaks were composed by metallic and oxide contributions. Thus it means that the native oxide thickness was lower than the depth analyzed by XPS, that is to say <5 nm [14]. Quantification of iron and chromium present in the native oxide layer was intended using a quantitative method which is not described in this paper. The thickness of the oxide layer was estimated to be about 3 nm and angular analyses revealed that the native oxide was duplex with an upper layer rich in iron and a lower layer rich in chromium. The detailed spectra recorded after reaching 550 °C (Fig. 4c, e, g) were composed by different contributions than the one presented at room temperature. Indeed iron peak was only composed by metallic contribution; the iron oxide contribution disappeared. Chromium peak was composed by metallic, oxide and nitride contributions. These contributions were confirmed by the analysis of the oxygen peak where chromium linked to oxygen contribution was present whereas there was no iron linked to oxygen. The analysis of the surface during the thermal ramp (not presented in this paper) showed that the transformation of the native oxide started at around 300 °C. These results clearly showed that oxygen from iron oxide reacted with chromium. As a consequence, as could be predicted by thermodynamics, chromium has more affinity for oxygen than iron and it reacts preferentially when the oxygen amount is very limited.

This phenomenon of oxidation of noble elements by native iron oxide was already described in the literature. On one hand, Es-Souni and Mosser [15] showed that during subsequent vacuum annealing at 450 °C, iron oxide was reduced and the surface was enriched with silicon oxide. On the other hand, Greeff [16] observed that the nature of the oxide present on 9Cr steel in UHV for 1,000 L is temperature dependent: below 400 °C it was composed by a duplex oxide layer with an external iron oxide and an internal chromium oxide whereas above 600 °C it was only made of chromium oxide.

Influence of the Thermal Ramp Rate

During this test campaign, the thermal ramp rate was increased from 2 to 15 °C/min in order to study the influence of this parameter on the oxidation of VM12 samples. On Fig. 5 are presented the GDOES profiles of samples after test 6 (CO_2 4.5) and test 7 (He 6.0).

In Fig. 5a, it can be observed that the oxide layer formed under CO_2 4.5 with a thermal rate of 15 °C/min was duplex with an external iron–chromium rich oxide layer and internal iron–chromium rich oxide layer richer in chromium (about 25 at.%). This oxide appeared to be different from the one formed under CO_2 4.5 at 2 °C/min (test 1), where no chromium was identified on the external oxide but similar to the one formed under CO_2 5.5 at 2 °C/min (test 2).

It should be noticed that the oxide formed after test 2 (2 °C/min in CO_2 5.5) was similar to the one formed at 2 °C/min in He 6.0 (not presented in this article) and composed by a duplex oxide with an internal oxide rich in chromium (20 at.%). Moreover, the GDOES profile of the sample oxidised under He 6.0 with a higher thermal ramp rate (Fig. 5b) revealed that the oxide layer was not a duplex oxide layer but only a single Cr rich oxide layer with a higher chromium enrichment of about 30 at.%. These results clearly showed the beneficial effect of high thermal ramp rate on the formation of chromium rich oxide.
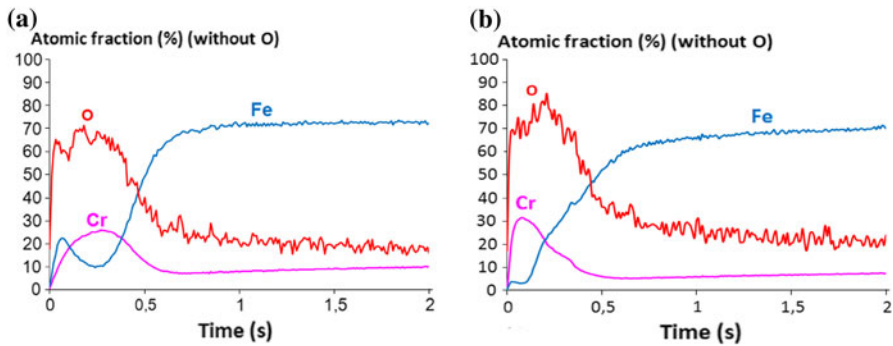
Fig. 5 GDOES profile of samples oxidised at 15 °C/min from room temperature to 550 °C under CO_2 4.5 (a test 6) and He 6.0 (b test 7)

Mechanism of Oxidation During the Initial Stages of Oxidation

In this part, a mechanism of oxidation explaining qualitatively the chromium content of the first oxide layers built during the first stage of oxidation is presented. It was supposed that O_2 react before CO_2 on the surface as suggested by our experimental results and that oxygen linked preferentially with chromium then with iron as suggested by in situ XPS oxidation tests. On Fig. 6 is presented a schematic illustration that defines the parameters involved in the model and their role on the nature of the oxide layer.

The mechanism of oxidation during the initial stage of oxidation must be able to explain both the effect of the oxygen amount in the gas phase and the effect of the thermal ramp rate on the chromium enrichment of the oxide layer. It is proposed that the chromium content of the initial oxide layer is function of two main parameters: the oxygen amount (N_O) and the chromium amount (N_{Cr}) available at the gas oxide interface to react together:

- The oxygen supply to the surface is determined by the amount of oxygen dissociated at the surface;
- The supply of chromium is assumed to be determined by the diffusion in the steel matrix as defined by Fick's law (the presence of a thin native oxide layer is supposed to be negligible).

When O_2 is dissociated at the surface, it reacts first with chromium available at the surface. If the amount of oxygen dissociated at the surface is higher to the one of chromium available at the surface then iron will be oxidized too. As a consequence, the amount of chromium (%Cr) in the first oxide scale is defined by the ratio N_{Cr}/N_O present at the surface at the first instants of oxidation.

X-ray photoelectron spectroscopy analyses have shown that oxidation reaction does not start before 300 °C. In our model, it must be assumed that N_{Cr} and N_O are defined for a time of accumulation Δt between T_S and 300 °C with T_S defined as the temperature at which dissociation of O_2 and Cr diffusion start to be not negligible (likely to be above 200 °C). This notion of time of accumulation Δt of the species on the surface is necessary to explain the chromium oxide enrichment with the
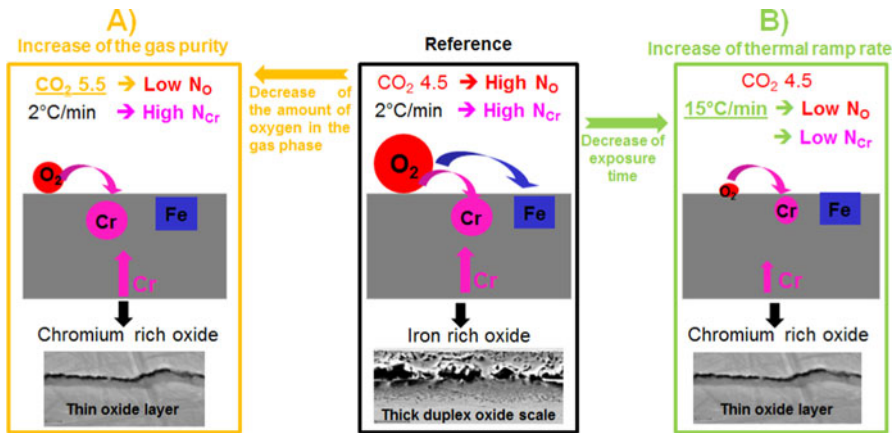
Fig. 6 Mechanism of oxidation during the initial stages of oxidation as a function of O_2 partial pressure in CO_2 and thermal ramp rate. N_O number of dissociated oxygen atoms (at/cm^{-2}), N_{Cr} number of chromium atoms (at/cm^{-2})

increase of the thermal ramp rate (Fig. 5). Once this model defined, let's try to explain our experimental results summarized in Fig. 6.

On the one hand, if the amount of oxygen impurities decreases (Fig. 6a), then the amount of dissociated oxygen N_O on the surface during Δt before the reaction at 300 °C decreases whereas the amount of chromium N_{Cr} accumulated during Δt does not change as compared to the reference situation (central columns in Fig. 6). As a consequence, N_{Cr}/N_O increases which means that the oxide would be richer in chromium. This is what was observed in Fig. 1 and in Fig. 3.

On the other hand, for a defined amount of O_2 impurities in the gas, if the thermal ramp rate increases (Fig. 6b) then the time of accumulation Δt between T_S and 300 °C decreases. As a consequence, N_{Cr} and N_O available at the surface both decrease. Because it is observed that the proportion of chromium the oxide layer increases with the thermal ramp rate increase (Fig. 5), it can be deduced that N_O decrease probably much stronger than N_{Cr}.

This oxidation model for the formation of the first oxide layers on low chromium steels is not trivial and has not been often described in the literature since little work paid attention to the initial stage of oxidation [9]. The next step of this work will be to quantitatively describe the observed chromium enrichment of the oxide layer and our selective oxidation model based on numerical expressions for N_O and N_{Cr}. It will be exposed in the next paper.

Conclusions

The present study showed that O_2 impurities present in the CO_2 gas phase reacted before CO_2 on the metallic surface during the first stage of oxidation. Depending on O_2 impurities amount, different oxide layers on 12 wt% Cr steel were observed. When the amount of O_2 was low, the selective oxidation of chromium led to the

formation of a thin chromium rich oxide layer, whereas the increase of the O_2 impurities resulted in the oxidation of both chromium and iron during the initial stage of oxidation. Increasing the thermal ramp rate appeared to be beneficial with respect to the chromium enrichment of the oxide layer. In order to explain all these observations, a "time of accumulation before reaction" for dissociated oxygen atoms and free reactive chromium atoms were introduced. The chromium content of the oxide layer is determined by the ratio N_{Cr}/N_O accumulated at the surface during this "time before reaction". This ratio in the first instants of oxidation is important for high purity CO_2 and high ramp rate and results in the formation of a chromium rich oxide layer as opposed to an iron rich oxide layer usually found in CO_2 media, which promotes the fast growth of a duplex oxide [1].

This study highlights the importance of the first stage of oxidation on the growth of this protective oxide layer and opens research tracks for corrosion behaviour improvement on ferritic–martensitic steels.

References

1. M. G. C. Cox, B. McEnaney and V. D. Scott, *Philosophical Magazine* **28**, 309 (1973).
2. C. S. Giggins and F. S. Pettit, *Oxidation of Metals* **14**, 363 (1980).
3. J. Pirón Abellán, T. Olszewski, G. H. Meier, L. Singheiser and W. J. Quadakkers, *International Journal of Materials Research* **101**, 287 (2010).
4. J. Pirón Abellán, T. Olszewski, H. J. Penkalla, G. H. Meier, L. Singheiser and W. J. Quadakkers, *Materials at High Temperatures* **26**, 63 (2009).
5. F. Rouillard, *Oxidation of Metals* **77**, 57 (2012).
6. F. Rouillard, *Oxidation of Metals* **77**, 27 (2012).
7. F. Rouillard, *Oxidation of Metals* **77**, 71 (2012).
8. C. T. Fujii and R. A. Meussner, *Journal of the Electrochemical Society* **114**, 435 (1967).
9. M. G. C. Cox, V. D. Scott and B. McEnaney, *Nature-Physical Science* **237**, 140 (1972).
10. G. H. Meier, K. Jung, N. Mu, N. M. Yanar, F. S. Pettit, J. Pirón Abellán, T. Olszewski, L. Nieto Hierro, W. J. Quadakkers and G. R. Holcomb, *Oxidation of Metals* **74**, 319 (2010).
11. S. Bouhieda, F. Rouillard, V. Barnier and K. Wolski, *Materials at High Temperatures* **29**, 151 (2012).
12. C. Leygraf and G. Hultquist, *Surface Science* **61**, 69 (1976).
13. D. Young, *High Temperature Oxidation and Corrosion of Metals*, (Elsevier, Amsterdam, 2008), p. 68.
14. Duc T.M., Techniques de l'ingénieur. P2625, 1.
15. M. Es-souni and A. Mosser, *Applied Surface Science* **35**, 219 (1988).
16. A. P. Greeff and Swart, *Corrosion Science* **42**, 1725 (2000).